JOURNAL OF SOLID STATE CHEMISTRY 27, 9–18 (1979)

Charge–Density Waves and Electron Localization in Vanadium Chalcogenides

C. F. VAN BRUGGEN, C. HAAS, AND G. A. WIEGERS

Laboratory of Inorganic Chemistry, Materials Science Center of the University, Nijenborgh 16, 9747AG, Groningen, The Netherlands

Received May 30, 1978

Transition metal compounds show interesting physical properties such as magnetism, metal–semiconductor transitions, valence disproportionation, charge–density waves, and metal–metal bonding. In this paper several of these effects are illustrated with recent experimental data of the vanadium chalcogenides and their sodium intercalates. The compounds Na_xVS_2 and Na_xVSe_2 occur in two crystal structure types. The type II compounds are antiferromagnetic semiconductors with localized *d* electrons and at low temperature a cooperative Jahn–Teller distortion. The type I compounds are metallic conductors which exhibit charge–density wave distortions (CDW). New data are reported on CDWs in VSe_2 (electron diffraction, transport properties). Finally, the relation between CDWs and metal–metal bonding is discussed.

Introduction

The metal atoms in transition metal compounds are characterized by the presence of a partly filled *d* shell. The nature of these *d* electrons is intermediate between that of well-localized electrons, such as the core electrons and the 4*f* electrons of the rare earths, and the nonlocalized outer electrons which are responsible for the chemical bonding. Another characteristic of transition metal atoms is the occurrence of these atoms in different valency states. These effects are responsible for the large variety of physical properties of transition metal compounds, such as magnetic properties, metal-semiconductor transitions, valence disproportionation, strong metal–metal bonding and charge–density waves (*1*). In this paper we illustrate several of these effects with recent experimental data of the vanadium chalcogenides and their sodium intercalates.

Localized and Itinerant *d* Electrons

The band theory of solids has been very successful for the description of the energy levels and the transport properties of normal nonmagnetic metals and semiconductors. In this theory, which is equivalent to molecular orbital theory for molecules, the electrons are assumed to move in an average potential due to the interaction with the nuclei and all other electrons. However, in this theory the correlation between the electrons is neglected, and the theory breaks down for those electrons for which correlation effects due to electron–electron interaction are important. This is the case for highly localized electrons.

A simple model Hamiltonian in which the electron–electron interaction is considered explicitly is the Hubbard Hamiltonian (*2*). For a linear array of equivalent atoms, each with a single nondegenerate orbital, this

0022-4596/79/010009-10$02.00/0

Hamiltonian is given by

$$\mathcal{H} = \sum_{\sigma} \sum_{i<j} t_{ij} c^{+}_{i\sigma} c_{j\sigma} + U \sum_{i} n_{i\sigma} n_{i,-\sigma}. \quad (1)$$

In this expression $c^{+}_{i\sigma}$ and $c_{i\sigma}$ are creation and annihilation operators for an electron with spin σ occupying an orbital at site i. The integral for the transfer of an electron from site i to site j is t_{ij}; the first term in (1) describes all effects such as overlap, taken into account in the usual one-electron band theory. The second term describes the correction due to the on-site interaction between the electrons. The number of electrons at site i with spin σ is $n_{i\sigma} = c^{+}_{i\sigma} c_{i\sigma}$. For one electron at i, say with spin σ, $n_{i\sigma} = 1$ and $n_{i,-\sigma} = 0$, and the second term in (1) vanishes. However, if there are two electrons at site i, $n_{i\sigma} = n_{i,-\sigma} = 1$, and the second term U represents the increase of the energy due to repulsion between the two electrons at site i.

The pseudoparticle spectrum of the Hubbard Hamiltonian consists of two bands (Fig. 1). For small values of the bandwidth W (which is proportional to the transfer integral t), the bands coalesce into two atomic levels with energies E_0 and $E_0 + U$, corresponding to atoms with one and two electrons, respectively. If there is one electron per site, the levels with energy E_0 are occupied, and those with energy $E_0 + U$ are empty; each atom has one electron and the crystal is nonconducting (Mott insulator). For larger bandwidths the atomic levels broaden and form energy bands. For a bandwidth W larger than a critical value ($W > 1.15U$) the two bands overlap, and form a single broad energy band. In this case the crystal is metallic, with itinerant electrons in a half-filled energy band. The system undergoes a transition from an insulating to a metallic state (Mott transition).

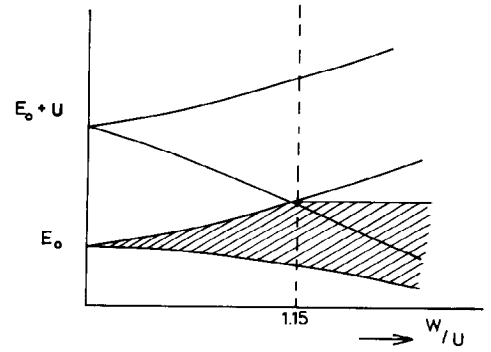

FIG. 1. Energy of the two Hubbard bands as a function of the bandwidth W. The metal–insulator transition is at $W/U = 1.15$.

The parameter U in the Hubbard Hamiltonian represents the effective on-site repulsion between the electrons. The value of U is strongly influenced by screening effects; especially in highly polarizable media (metals, or compounds with highly polarizable anions) this screening leads to a strong reduction of U (*3*). The polarization also leads to a strong reduction of the transfer integrals (*4*).

These considerations explain qualitatively the occurrence of insulating transition metal oxides (MnO, NiO, CoO) with localized d electrons. In other transition metal oxides (TiO, VO, ReO_3) the d electrons are itinerant and cause metallic conductivity (*5, 6*).

Transitions from localized to itinerant behavior are observed in several transition metal compounds, such as V_2O_3 and NiS (*7*). We discuss here recent data on localized and itinerant d electrons in vanadium chalcogenides Na_xVS_2 and Na_xVSe_2 (*8–12*). The structure of these compounds consists of sandwich layers VS_2 and VSe_2, with Na atoms intercalated in the van der Waals gap between the sandwich layers. Two types of crystal structures are observed. In the type I compounds, the coordination of the Na atoms is trigonal-prismatic; in type II compounds the Na atoms are surrounded by a trigonally distorted octahedron of chalcogen atoms. It is found that this difference in structure has a large influence on the properties of the vanadium d electrons (Table I, Fig. 2). The type I compounds are metallic and Pauli-paramagnetic and have itinerant d

TABLE I

PROPERTIES OF Na_xVS_2 AND Na_xVSe_2

	Na_xVS_2		Na_xVSe_2	
	Type I	Type II	Type I	Type II
Coordination of V	Octahedral	Octahedral	Octahedral	Octahedral
Coordination of Na	Trigonal prismatic	Octahedral	Trigonal prismatic	Octahedral
Composition x	0.3–1.0	1.0	0.5–0.6	1.0
a (Å)	3.346 ($x = 0.6$)	3.566	3.482 ($x = 0.6$)	3.735
c (Å)	21.02 ($x = 0.6$)	19.68	22.21 ($x = 0.6$)	20.639
Electrical conduction	Metallic	Semiconductor	Metallic	Semiconductor
Magnetic property	Pauli-paramagmetic	AF	Pauli-paramagmetic	AF
Distortion	CDW	Jahn-Teller	CDW	Jahn-Teller

electrons. The electrical properties of these compounds (electrical resistivity, Hall effect, thermoelectric power) show anomalies which are due to charge-density wave (CDW) distortions at low temperatures. These distortions were observed directly by electron diffraction. The type II compounds have localized d electrons, with localized magnetic moments characteristic of $V^{3+}(3d)^2$ ions, and show a semiconducting behavior. The V–V distances in the hexagonal layers (the crystallographic a axis) are shorter in the metallic type I compounds; this is as expected: A short V–V distance corresponds to a large transfer integral and therefore to itinerant d electrons. The magnetic moments of the vanadium atoms of the type II compounds order antiferromagnetically below $T_N = 49.0°K$ (the maximum of χ is at 75.0°K, the steepest descent at 49.0°K) for $NaVS_2$ (Fig. 2), and $T_N = 49.7°K$ (maximum of χ 50.4°K, steepest descent at 49.7°K) for $NaVSe_2$. The transition at T_N is a first-order phase transition. Below T_N the crystal lattice is distorted due to a cooperative Jahn–Teller effect caused by

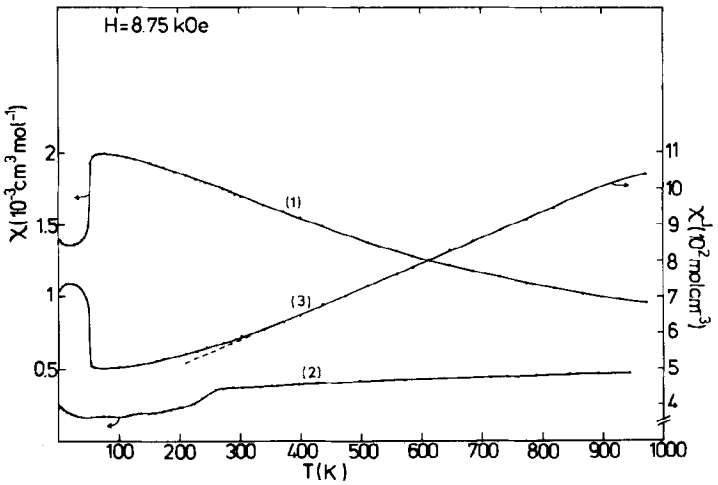

FIG. 2. Molar magnetic susceptibility (left axis) and reciprocal susceptibility (right axis) vs temperature at $H = 8.75$ kOe of two different forms of $NaVS_2$; (1) χ of type II; (2) χ of type I; (3) χ^{-1} of type II.

the orbitally degenerate ^3E_g state of the V^{3+} $(3d)^2$ ions in a trigonally distorted octahedron. The distortion is driven by the coupling between the localized electronic state ^3E_g and the crystal lattice strain in $D_{3d}: {}^3E_g \otimes \varepsilon_g$; it lowers both the point- and space-group symmetry from D_{3d} to C_{2h}.

Charge–Density Waves

Several metallic crystals undergo phase transitions which are driven by instabilities of the conduction electrons. These transitions lead to a charge–density wave, defined as a static periodic change of the electron density coupled with a periodic lattice distortion (*13*). The change of the electron density will generally cost electron–electron repulsive energy; however, the positive ions in the crystal will move in response to the new charge distribution, and this lowers the energy. If the electron–phonon coupling is sufficiently strong, the state of lowest energy is a charge–density wave.

A distortion of the lattice with a periodicity described by a wave vector q leads to a change of the effective potential $\delta V_q \exp(iqr)$ for the electrons, and this produces a change of the electron density

$$\Delta\rho(r) = \chi(q)\,\delta V_q\, e^{iqr}, \tag{2}$$

in which $\chi(q)$ is the response function of the conduction electrons. For a free electron gas $\chi_0(q)$ is given by

$$\chi_0(q) = \sum_k \frac{f_k(1-f_{k+q})}{\varepsilon_{k+q}-\varepsilon_k}, \tag{3}$$

where ε_k is the energy of a state with wave vector k, and f_k is the Fermi occupation function

$$f_k = \frac{1}{e^{(\varepsilon_k-\varepsilon_F)/kT}+1}, \tag{4}$$

where $\sum_F$ is the Fermi energy. The shape of the $\chi_0(q)$ vs q curve depends strongly on the dimensionality (Fig. 3). For a three-dimensional metal $\chi_0(q)$ has a weak singularity at

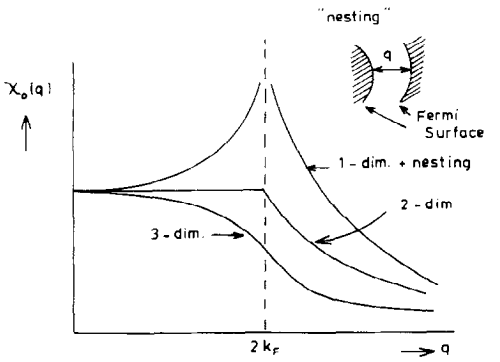

FIG. 3. Response function $\chi_0(q)$ of one-, two-, and three-dimensional free electron gases; k_F is the wave vector of the electrons at the Fermi level. Nesting: parallel parts of the Fermi surface connected by q.

$q = 2k_F$; for a two-dimensional metal the singularity is more pronounced; and for a one-dimensional metal $\chi_0(q)$ diverges at $q = 2k_F$. The consequence is that a one-dimensional metal is unstable for a distortion of periodicity $q = 2k_F$. For a half-filled band $k_F = \pi/2a$, if a is the lattice parameter, and the distortion corresponds to a doubling of the unit cell (a dimerization); this is the well-known Peierls instability.

Even if the crystal is not strictly one- or two-dimensional, it is possible that certain parts of the Fermi surface have a one- or two-dimensional character. A large value of $\chi(q)$ is obtained if the Fermi surface contains large areas connected by q with parallel tangent planes. This is the so-called nesting, responsible for the CDWs in two-dimensional metals (Fig. 3). The periodicity of the lattice distortion, corresponding to the charge–density wave, produces gaps at the Fermi surface, and this leads to the destruction of certain pieces of the Fermi surface.

An interesting feature is the occurrence of incommensurate CDWs. Generally the period of the CDW is determined by (the maximum of) $\chi(q)$, i.e., by the properties of the Fermi surface. As a consequence the lattice distortion is not necessarily commensurate with the undistorted lattice.

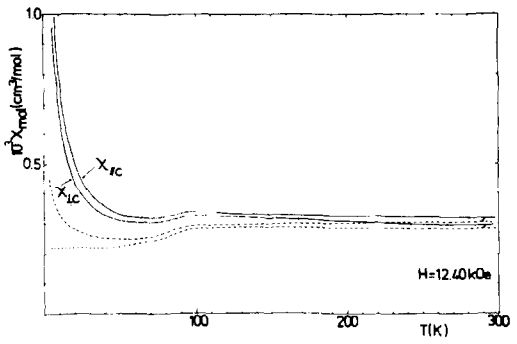

FIG 4. Molar magnetic susceptibility of VSe_2 single crystals (composition $V_{1.015}Se_2$) for a field $H = 12.4$ kOe parallel ($\chi_\parallel$) and perpendicular ($\chi_\perp$) to the trigonal axis. The solid lines represent the data as measured; the broken lines are corrected for 0.23% paramagnetic $V^{2+}(3d)^3$ ions.

CDWs have been observed in many transition metal chalcogenides with a layer structure, such as TaS_2, $NbSe_2$, etc. (*13*). Here we report some new data on CDWs in vanadium diselenide VSe_2 (*14*).

$1T$–VSe_2 has a layer-type structure, with V in octahedral sites. The crystals are metallic and Pauli-paramagnetic (Figs. 4, 5) (*15, 16*). The electrical and magnetic properties show several anomalies as a function of the temperature. These anomalies are small, but real and reproducible, and are manifestations of phase transitions due to CDWs. This was confirmed by electron diffraction studies of thin crystals, shown in Fig. 6 (*14*). At low temperatures, first a diffuse scattering, accompanied by an incommensurate pattern, is observed which transforms into a $3a \times 3a$ supercell. At still lower temperatures another incommensurate CDW develops with $q = 0.41a^*$ in the $\langle 11\bar{2}0 \rangle$ direction; this transforms, probably at about 100°K, into an $a7^{1/2} \times a7^{1/2}$ supercell ($q = (1/7^{1/2}) \times a^* = 0.378a^*$ in the $\langle 12\bar{3}0 \rangle$ direction).

Attempts have been made to correlate observed CDWs with the Fermi surface obtained from band structure calculations. For $1T$–VSe_2 preliminary band structure calculations have been reported (*17, 18*), and the observed CDW vector q is not incompatible with the computed Fermi surface. However, the observed distortion patterns of $1T$–VSe_2 are too complicated to make a direct interpretation possible.

Additional information for the interpretation of CDWs can be obtained from a comparison of Hall effect and thermoelectric

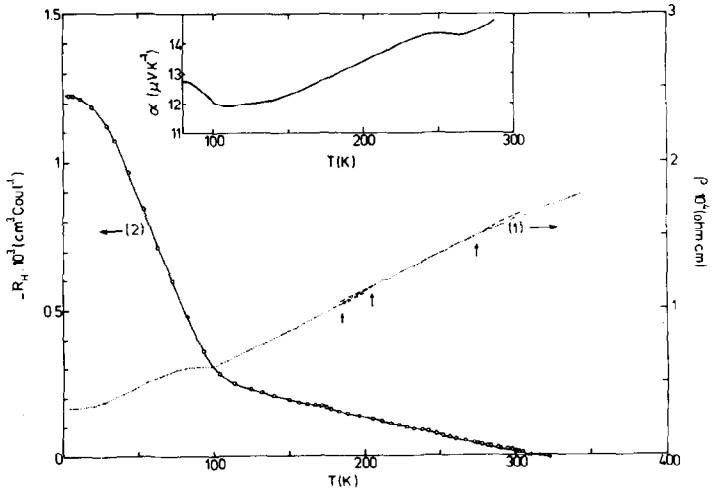

FIG. 5. Electrical resistivity ρ (curve 1), Hall coefficient R_H (curve 2), and thermoelectric power α (inset) of single crystals of $1T$-VSe_2. The electrical current is parallel and the magnetic field is perpendicular to the basal plane. The arrows indicate regions where minor anomalies of the temperature dependence are observed.

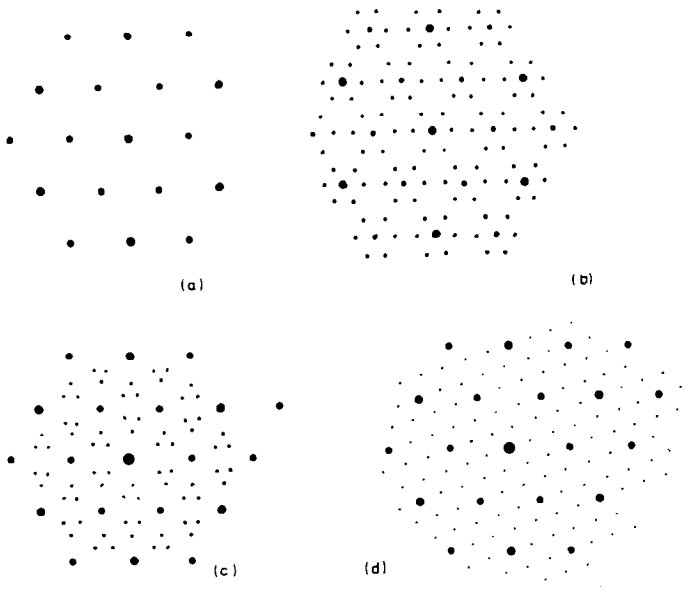

FIG. 6. Electron diffraction patterns of $1T$-VSe_2; (a) undistorted; (b) $3a \times 3a$ superstructure; (c) incommensurate structure with $q = 0.41a^*$ in the $\langle 11\bar{2}0 \rangle$ direction; (d) $a7^{1/2} \times a7^{1/2}$ superstructure.

power data. In the case of mixed conduction (by electrons and holes, or by carriers with small and large effective mass) the Hall effect is dominated by the mobile carriers with the small effective mass, whereas the thermoelectric power is characteristic for carriers with a large effective mass. In $1T$-VSe_2 the Hall effect is negative, and the Seebeck effect is positive, indicating a mixed conduction with light electrons and heavy holes. The various CDW transitions have different effects on R_H and α. For example, the low-temperature transition which corresponds to the occurrence of the $a7^{1/2} \times a7^{1/2}$ structure results in a large increase of R_H and but a small increase of α. Therefore this transition apparently corresponds to the destruction of pieces of the Fermi surface which describe light electrons.

Charge-Density Waves and Metal–Metal Bonding

The compounds for which CDWs have been reported are metallic transition metal compounds, with a narrow partly filled d band. For example, in $1T$-VSe_2, the vanadium atoms V^{4+} have a $(3d)^1$ configuration, and the electrical conductivity is due to the d electrons. The d electrons are also responsible for the occurrence of metal–metal bonding in several transition metal compounds. For example, in many compounds of Nb^{4+}, the Nb atoms are present in Nb–Nb pairs, with a covalent metal–metal bond due to overlap of $4d$ orbitals. In this section we discuss the relation between the CDW and metal–metal bonding (*4, 19*).

First we consider a linear chain of equally spaced atoms (spacing a). We assume the presence of interactions which keep the total length of the chain of $N+1$ atoms fixed to Na. The interaction between the atoms is represented by an attractive potential $\phi(r)$, which describes the chemical bonding between the atoms. The energy of the undistorted chain is $E_0 = N\phi(a)$. For a dimerized chain, with alternating short, strong bonds of length $a-u$, and long, weak bonds of

length $a+u$, the energy is $E_d = \frac{1}{2}N\{\phi(a-u)+\phi(a+u)\}$. The dimerized chain is stable if $E_d < E_0$, or for $(\partial^2\phi/\partial r^2)_{r=a} < 0$ (Fig. 7). This simple example shows that the dimerization of a linear chain is not necessarily due to a Fermi surface instability in a metallic crystal (Peierls instability). A sufficient condition for dimerization is that the energy of a short and a long chemical bond be less than the energy of two bonds of intermediate length.

We now discuss the case of a simple two-dimensional hexagonal lattice, as it occurs in many transition metal compounds. The overall dimensions of the lattice are mainly determined by repulsive interactions between the nonmetal atoms. We will show that a simple isotropic attractive interaction between the metal atoms can lead to complicated distortion patterns similar to those observed in layer compounds.

In the model we consider an interaction $\phi_0(r)$ which keeps each metal atom bound to a particular lattice site. We also introduce an attractive interaction between nearest-neighbor metal atoms $\phi_1(r)$. An arbitrary displacement of metal atom n from its lattice site $R_n^0 = n_1 a + n_2 b$ (a and b are the lattice vectors of the hexagonal unit cell; n_1 and n_2 are integers) is written as

$$R_n - R_n^0 = \sum_k u_k e^{ikR_n^0}, \tag{5}$$

i.e., as a sum of periodic lattice distortions with wave vector k. The total energy is

$$E = \sum_n \phi_0(|R_n - R_n^0|) + \sum_n \sum_s \phi_1(|R_{n+s} - R_n|). \tag{6}$$

The sum is over all nearest neighbors of site n: $s = \pm a, \pm b, \pm(a-b)$. The energy can be expanded in a power series in the atomic displacements:

$$E = \sum_k a_k |u_k|^2 + \text{higher-order terms}. \tag{7}$$

The coefficients of this expansion can be expressed in terms of the derivatives of ϕ_0 and ϕ_1. The stable lattice distortions are obtained by minimizing the energy with respect to the wave vector k and the angle ψ_k which the atomic displacements make with the a axis. (ψ_k is the angle between u_k and a.) In this manner several solutions are obtained:

(A) the undistorted state;

(B) three equivalent solutions $k_1 = (0\,\frac{1}{2})$,

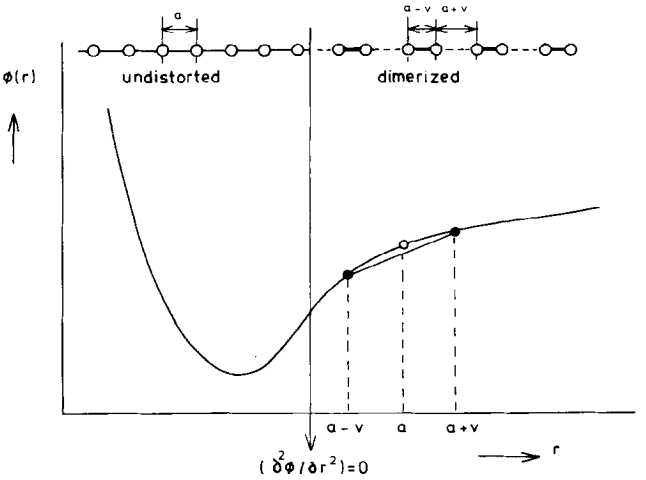

FIG 7. Interaction function $\phi(r)$ between metal atoms. Dimerization of a linear chain occurs if $\phi(a+u)+\phi(a-u) < 2\phi(a)$.

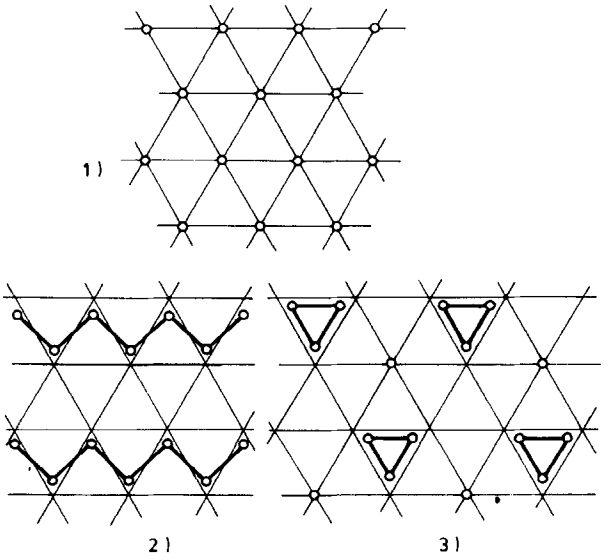

FIG. 8. Lattice distortions of a two-dimensional hexagonal lattice: (1) undistorted; (2) MnP-type distortion $k_1 = (0\,\frac{1}{2})$, $\psi = 90°$, with zig-zag chains of metal atoms; (3) lt. NbS-type structure, with triangles and isolated atoms. This solution is a superposition of three MnP-type distortions.

$\psi = 90°$; $k_2 = (\frac{1}{2}\,0)$, $\psi = -30°$; $k_3 = (\frac{1}{2}\,\frac{1}{2})$, $\psi = 30°$; these solutions correspond to distortions of MnP type, with zig-zag chains of metal atoms (Fig. 8);

(C) more complicated solutions.

The energy of linear combinations of equivalent solutions is the same as far as quadratic terms are concerned, but this is not so for higher-order terms. For solutions (B) the third-order terms vanish, and the fourth-order terms are

$$E_4 = Nu^4\{D_1 + D_2(\gamma_2^2\gamma_3^2 + \gamma_3^2\gamma_1^2 + \gamma_1^2\gamma_2^2)\}, \tag{8}$$

where $u_{k_i} = u\gamma_i$ is the amplitude of the distortion with wave vector k_i, and $\gamma_1^2 + \gamma_2^2 + \gamma_3^2 = 1$. The coefficients D_1 and D_2 can be expressed in terms of the higher derivatives of ϕ_0 and ϕ_1. By minimizing the energy with respect to γ_1, γ_2, and γ_3, the most stable solutions are obtained. It is found that the MnP-type distortion ($\gamma_1 = 1$, $\gamma_2 = \gamma_3 = 0$) is stable for $D_2 > 0$, but for $D_2 < 0$, a linear combination $\gamma_1 = \gamma_2 = \gamma_3 = 1/3^{1/2}$ has a lower energy. This distortion is sketched in Fig. 8; it consists of triangles of metal atoms and isolated atoms, and it is the structure observed in the low-temperature form of NbS.

It is found that if only interactions with nearest neighbors are taken into account, solutions (B) (MnP type, or lt. NbS type) always have a lower energy than the more complicated solutions (C). Therefore the MnP-type and lt. NbS-type distortions are the natural distortions for nearest-neighbor bonding. This explains the frequent occurrence of especially the MnP-type structure in many transition metal chalcogenides (*20*).

The more complicated patterns of distortion can be stabilized by interactions with more distant neighbors. Also among these solutions are incommensurate distortions. In Fig. 9 a number of these solutions are shown. Each distortion has trigonal symmetry and is a superposition of a number of equivalent distortions. The simplest distortion consists of triangles of atoms and is described by a superposition of distortions with $k_1 = (\frac{2}{3}\,\frac{1}{3})$ and $k_2 = (\frac{1}{3}\,\frac{2}{3})$. This structure, which has an

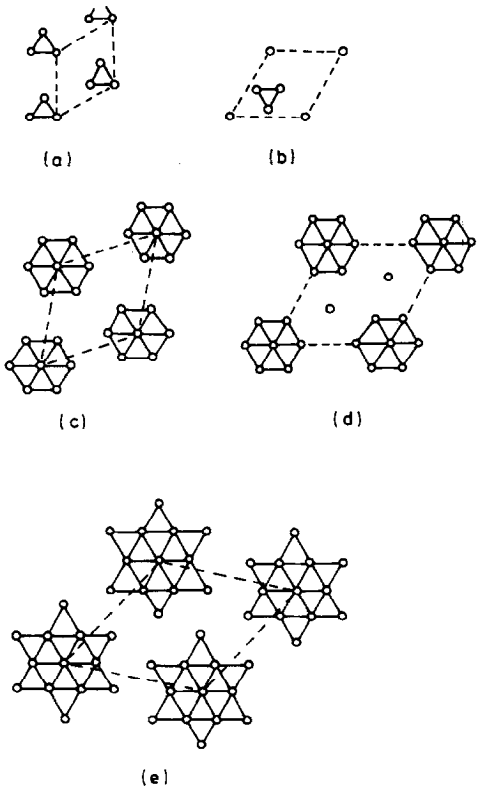

FIG. 9. Trigonal distortions of a hexagonal lattice, due to the clustering of atoms. The unit cells are indicated by dotted lines. (a) $a3^{1/2} \times a3^{1/2}$ cell; FeS. (b) $2a \times 2a$ cell; lt. NbS. (c) $a7^{1/2} \times a7^{1/2}$ cell; $1T$–VSe_2. (d) $3a \times 3a$ cell; $1T$–VSe_2, $2H$–$TaSe_2$, $2H$–$NbSe_2$. (e) $a13^{1/2} \times a13^{1/2}$ cell; $1T$–TaS_2, $1T$–$TaSe_2$.

$a3^{1/2} \times a3^{1/2}$ unit cell, has been observed in FeS (*21*). The low-temperature NbS-type structure also has triangles, but isolated metal atoms in addition. A similar relation exists between the $3a \times 3a$ and $a7^{1/2} \times a7^{1/2}$ structures of $1T$–VSe_2; in both structures there are clusters of 7 metal atoms, in the $3a \times 3a$ structure there are also isolated atoms. These, and also the more complicated distortions with a cluster of 13 atoms, are the distortions reported for the CDWs of the layered transition metal dichalcogenides (*13, 22*).

These considerations show that the distortions can be regarded as also due to metal–metal bonding, leading to the clustering of the atoms. Distortions of this type are frequent in compounds with metal atoms which show a strong tendency to form clusters also in molecular compounds. Examples are the halides of Mo, Ta, and Nb, such as Mo_6Cl_{12} and Ta_6Cl_{14}, which contain octahedra of transition metal atoms, with short metal–metal distances and strong metal–metal bonds (*23*).

Finally we remark that the clustering of metal atoms and the periodic lattice distortions corresponding to the charge-density waves are not independent phenomena. The Fermi surface instability combined with electron–phonon interaction and the chemical bonds expressed in terms of an effective attractive interaction between the metal atoms are both descriptions of the interactions between metal atoms via the partly filled *d*-like conduction band.

References

1. J. B. GOODENOUGH, "Magnetism and the Chemical Bond," Interscience, New York (1963).
2. J. HUBBARD, *Proc. Roy. Soc., Ser. A* **276**, 238 (1963); **277**, 237 (1964); **281**, 401 (1964).
3. G. A. SAWATZKY, P. I. KUINDERSMA, AND J. KOMMANDEUR, *Solid State Commun.* **17**, 569 (1975).
4. C. HAAS, *Curr. Topics Mater. Sci.*, in press.
5. D. ADLER, *Solid State Phys.* **21**, 1 (1968).
6. J. B. GOODENOUGH, in "Progress in Solid State Chemistry" (H. Reiss, Ed.), Pergamon, Oxford (1971).
7. N. F. MOTT, "Metal–Insulator Transitions," Taylor & Francis, London (1974).
8. G. A. WIEGERS, R. VAN DER MEER, H. VAN HEININGEN, H. J. KLOOSTERBOER, AND A. J. A. ALBERINK, *Mater. Res. Bull.* **11**, 1261 (1974).
9. J. R. BLOEMBERGEN, R. J. HAANGE, AND G. A. WIEGERS, *Mater. Res. Bull.* **12**, 1103 (1977).
10. J. R. BLOEMBERGEN, R. J. HAANGE, G. A. WIEGERS, AND C. F. VAN BRUGGEN, Ext. Abstr. Vth Int. Conf. Solid Comp. Transition Elements, Uppsala, 1976, p. 60.
11. G. A. WIEGERS AND C. F. VAN BRUGGEN, *Physica B* **86-88**, 1009 (1977).

12. C. F. VAN BRUGGEN, J. R. BLOEMBERGEN, A. J. A. BOS-ALBERINK, AND G. A. WIEGERS, *J. Less Common Metals* **60**, 259 (1978).
13. J. A. WILSON, F. J. DISALVO, AND S. MAHAJAN, *Advan. Phys.* **24**, 117 (1975).
14. J. VAN LANDUYT, G. A. WIEGERS, AND S. AMELINCKX, *Phys. Strat. Sol.* $A\mathbf{4}^{6}$, 479 (1978).
15. C. F. VAN BRUGGEN AND C. HAAS, *Solid State Commun.* **20**, 251 (1976).
16. C. F. VAN BRUGGEN, to be published.
17. G. WEXLER, A. M. WOOLLEY, AND N. DORAN, *Nuovo Cimento B* **38**, 571 (1977).
18. A. M. WOOLEY AND G. WEXLER, *J. Phys. C.* **10**, 2601 (1977).
19. C. HAAS, *Solid State Commun., Solid State Commun.* **26**, 709 (1978).
20. H. F. FRANZEN, C. HAAS, AND F. JELLINEK, *Phys. Rev. B* **10**, 1248 (1974).
21. J. M. COEY, H. ROUX-BUISSON, AND R. BRUSETTI, *J. Phys. (Paris) C* **4**, 1 (1976).
22. R. BROUWER, thesis, Groningen, 1978.
23 R. B. KING, *Progr. Inorg. Chem.* **15**, 287 (1972).